

Two Types of Thalamocortical Projections from the Motor Thalamic Nuclei of the Rat: A Single Neuron-Tracing Study Using Viral Vectors

Eriko Kuramoto¹, Takahiro Furuta¹, Kouichi C. Nakamura^{1,2}, Tomo Unzai¹, Hiroyuki Hioki¹ and Takeshi Kaneko^{1,2}

¹Department of Morphological Brain Science, Graduate School of Medicine, Kyoto University, Kyoto 606-8501, Japan and ²Core Research for Evolutionary Science and Technology, Japan Science and Technology Agency, Kawaguchi 332-0012, Japan

The axonal arborization of single motor thalamic neurons was examined in rat brain using a viral vector expressing membrane-targeted palmitoylation site-attached green fluorescent protein (palGFP). We first divided the ventral anterior-ventral lateral motor thalamic nuclei into 1) the rostromedial portion, which was designated inhibitory afferent-dominant zone (IZ) with intense glutamate decarboxylase immunoreactivity and weak vesicular glutamate transporter 2 immunoreactivity, and 2) the caudolateral portion, named excitatory subcortical afferent-dominant zone (EZ) with the reversed immunoreactivity profile. We then labeled 38 motor thalamic neurons in 29 hemispheres by injecting a diluted palGFP-Sindbis virus solution and isolated 10 IZ and EZ neurons for reconstruction. All the reconstructed IZ neurons widely projected not only to the cerebral cortex but also to the neostriatum, whereas the EZ neurons sent axons almost exclusively to the cortex. More interestingly, 47–66% of axon varicosities of IZ neurons were observed in layer I of cortical areas. In contrast, only 2–15% of varicosities of EZ neurons were found in layer I, most varicosities being located in middle layers. These results suggest that 2 forms of information from the basal ganglia and cerebellum are differentially supplied to apical and basal dendrites, respectively, of cortical pyramidal neurons and integrated to produce a motor execution command.

Keywords: layer I, motor thalamic neurons, Sindbis viral vector, single-neuron tracing, ventral anterior-ventral lateral complex

Introduction

Motor thalamic nuclei, mainly composed of ventral anterior (VA) and ventral lateral (VL) nuclei, receive massive afferents from the basal ganglia and cerebellum and project their axons to motor cortical areas (for review, see Groenewegen and Witter 2004; Jones 2007). Although the ventromedial nucleus receives dense afferents from the basal ganglia and may be considered to be a part of the motor thalamus, the present study has been concentrated on the VA-VL complex. In the primates, the VA and VL are clearly distinguished from each other, and further, the VL is divided into 2 major divisions, anterior (VLo or VL_a) and posterior portions of VL (VL_c or VL_p), on the basis of the cytoarchitecture (Jones 2007). Roughly speaking, these subdivisions, VA, VLo, and VL_c, receive afferents from the substantia nigra pars reticulata, internal segment of the globus pallidus, and deep cerebellar nuclei, respectively, and these afferents overlap little, if at all, with one another. In the rat brain, the VA and VL are known to constitute a single nuclear mass as the VA-VL complex because the cytoarchitecture is indistinguishable between the VA and VL (Jones 2007). However, it is likely that the rat VA-VL

complex is functionally segregated at least into 2 portions as the monkey motor thalamus because cerebellar and basal ganglia afferents were rather separately distributed in the caudolateral (Faull and Carman 1978; Angaut et al. 1985; Deniau et al. 1992) and rostromedial portions of the VA-VL complex (Deniau et al. 1992; Sakai et al. 1998; Bodor et al. 2008), respectively. The information of the basal ganglia and cerebellar circuits should be integrated for the generation of appropriate motor activity. Because the 2 pieces of information are not extensively converged in the subcortical regions including the thalamic nuclei, the integration is considered to occur in the cerebral cortex. As a possible step of the integration, thalamocortical projections conveying the basal ganglia and cerebellar information are to be examined.

Thalamocortical afferent fibers from the VA-VL complex have been studied using the axonal degeneration and anterograde tracer methods in the rat (Yamamoto et al. 1990), cat (Strick and Sterling 1974; Shinoda and Kakei 1989), and monkey brains (Nakano et al. 1992; McFarland and Haber 2002). These techniques were not suitable for revealing the fine organization of the 2 kinds of thalamocortical projections conveying the basal ganglia and cerebellar information, and thus, the morphological analysis of the 2 projections at a single axon level was necessary. However, only a few studies were reported on the single-axon fibers emitted from VA-VL neurons by the Golgi impregnation (Asanuma and Fernandez 1974), intra-axonal staining (Deschênes and Hammond 1980; Shinoda 1987), or small biocytin injection to the VA-VL complex (Aumann et al. 1998). The origin of the cortical afferents was unknown in the Golgi impregnation study, and the cortical axonal arborization labeled with extracellular biocytin injection appeared incomplete when compared with the intra-axonal labeling. Because the reported intra-axonally labeled fibers responded orthodromically to VL stimulation and monosynaptically to cerebellothalamic stimulation, they were considered to belong to the cerebellothalamocortical system. However, because the axons were not completely labeled retrogradely from the injection site in the intra-axonal staining, the whole axonal arborization of single VL neurons might be missed if a neuron had main axonal branches between the injection site and cell body. Furthermore, no morphological information is available for single neurons transmitting the basal ganglia information to motor areas. Thus, it still remains unknown at a single-neuron level how different the thalamocortical projections transmitting the basal ganglia information and conveying the cerebellar information are and how they are integrated in motor areas.

We recently developed a replication-deficient Sindbis viral vector (Furuta et al. 2001), which was designed to express

palmitoylation site-attached green fluorescent protein (palGFP) and used as an anterograde tracer of neurons (Nakamura et al. 2004; Ito et al. 2007). The vector was a highly sensitive anterograde tracer because infected neurons produced an enormous amount of palGFP under the strong subgenomic promoter of the virus (Bredenbeek et al. 1993), and the palGFP was targeted to plasma membrane including axonal membrane by the addition of long fatty acid, palmitic acid, to the protein (Moriyoshi et al. 1996). This is the reason that, in the present study, we applied the palGFP-Sindbis virus vector to single-neuron labeling in the VA-VL complex. If the viral solution was enough diluted, only 1 to 3 neurons would be infected in the thalamic nuclei and their axonal arborization could be isolated for the full reconstruction. The aim of the present study was to examine morphological differences between neurons transmitting the cerebellar information and those conveying the basal ganglia information to motor areas by completely visualizing their axonal arborization with the new technique.

Materials and Methods

Animals

Adult male Wistar rats, weighing 250–350 g, were used in the present study. Experiments were conducted in accordance with the guidelines of the animal care by Institute of Laboratory Animals, Faculty of Medicine, Kyoto University. All efforts were made to minimize the suffering and number of animals used in the present study.

Injection of Sindbis Viral Vector and Fixation

Forty-nine rats were anesthetized by intraperitoneal injection of chloral hydrate (35 mg/100 g body weight). For single-neuron labeling, 3–6 × 10² infectious units (IU) of palGFP-Sindbis viral vectors (Furuta et al. 2001) in 0.3 µL of 5 mM sodium phosphate (pH 7.4)-buffered 0.9% saline (PBS) containing 0.5% bovine serum albumin (BSA) were injected into the VA-VL complex of the thalamus (2.6–3.0 mm posterior to the bregma, 1.8–2.0 mm lateral to the midline, and 5.3–6.0 mm deep from the brain surface) by pressure through a glass micropipette attached to Picospritzer II (General Valve Corporation, East Hanover, NJ). The virus-injected rats survived for 50–55 h after the injection. For the control experiments using another 3 rats, we also injected a larger amount (2 × 10⁷ IU/µL × 0.5 µL = 10⁷ IU) of Sindbis viral vectors expressing GFP into the VA-VL complex and allowed a survival time of 50–96 h.

The 52 virus-injected rats and 2 untreated rats were anesthetized with chloral hydrate (70 mg/100 g) and perfused transcardially with 200 mL of PBS, followed by 200 mL of 3% formaldehyde, 75%-saturated picric acid, and 0.1 M Na₂HPO₄ (adjusted with NaOH to pH 7.0). The brains were then removed, cut at the midline into 2 hemispheric blocks, and postfixed for 4 h at room temperature with the same fixative. After cryoprotection with 30% sucrose in PBS, the blocks were cut into 40-µm-thick parasagittal sections on a freezing microtome, and the sections were collected serially in PBS.

Characterization of palGFP-Expressing Thalamic Neurons

The sections including the injection site were observed under epifluorescent microscope Axiophot (Zeiss, Oberkochen, Germany) to find thalamic neurons infected with the virus. All the following incubations were performed at room temperature and followed by a rinse with PBS containing 0.3% Triton X-100 and 0.02% merthiolate (PBS-X). The sections containing palGFP-positive thalamic neurons were incubated overnight with 2 µg/mL mouse monoclonal immunoglobulin G (IgG)_{2a} to recombinant glutamic acid decarboxylase 67 (GAD67; MAB5406, Chemicon, Temecula, CA) in PBS-X containing 0.12% lambda-carrageenan, 0.02% sodium azide, and 1% donkey serum (PBS-XCD) and then for 4 h with 1 µg/mL Alexa Fluor 647-conjugated

anti-(mouse IgG) goat antibody (Molecular Probes, Eugene, OR) in PBS-XCD. Under an LSM5 PASCAL confocal laser-scanning microscope (Zeiss), the location of palGFP-labeled neurons was examined in reference to GAD67 immunoreactivity as described in Results. Further, the sections containing palGFP-labeled neurons were incubated for 2 h with 10 µg/mL of propidium iodide in PBS-X, and the location of the labeled neurons was reexamined in reference to Nissl-like staining with propidium iodide.

Immunoperoxidase Staining for GFP

GFP immunoreactivity was visualized by combining the avidin-biotinylated peroxidase complex (ABC) method with the biotinylated tyramine (BT)-glucose oxidase (GO) amplification, which was newly developed in the present study. All the serial sections containing 3 or less palGFP neurons in a hemisphere and control sections of GFP-Sindbis virus-injected rats were incubated overnight with 0.4 µg/mL affinity-purified rabbit antibody to GFP (Tamamaki et al. 2000; Nakamura et al. 2008) in PBS-XCD. After a rinse with PBS-X, the sections were incubated for 2 h with 10 µg/mL biotinylated anti-(rabbit IgG) goat antibody (Vector, Burlingame, CA) and then for 1 h with ABC (1:100; Elite variety, Vector) in PBS-X. After a rinse in 0.1 M sodium phosphate buffer (PB; pH 7.4), the sections were incubated for 30 min in the BT-GO reaction mixture containing 1.25 µM BT, 3 µg/mL of GO (nacalai tesque, Kyoto, Japan; 259 U/mg), 2 mg/mL of beta-D-glucose, and 1% BSA in 0.1 M PB (pH 7.4) (for further detail, see Supplementary Data), followed by a wash with PBS. Subsequently, the sections were again incubated for 1 h with ABC in PBS-X, and the bound peroxidase was finally developed brown by reaction for 30–60 min with 0.02% diaminobenzidine (DAB)-4HCl and 0.0001% H₂O₂ in 50 mM Tris-HCl, pH 7.6. All the above incubations and reactions were performed at room temperature. All the stained sections were serially mounted onto the gelatinized glass slides, dried up, dehydrated in an ethanol series, cleared in xylene, and finally coverslipped. After camera lucida reconstruction of palGFP-labeled neurons, the sections were counterstained for Nissl with 0.2% cresyl violet to determine cytoarchitecture of the cerebral cortex.

Immunoperoxidase Staining for Calbindin D28k, GAD67, and VGluT2 in Control Sections

The control sections of untreated rats were incubated with 1 µg/mL mouse monoclonal antibody to GAD67, 1 µg/mL mouse monoclonal IgG₁ to calbindin D28k (C9848; Sigma, St Louis, MO), or 1 µg/mL affinity-purified rabbit antibody to vesicular glutamate transporter 2 (VGluT2; Hioki et al. 2003). They were subsequently incubated for 2 h with 10 µg/mL biotinylated anti-(mouse IgG) donkey antibody (Chemicon) or anti-(rabbit IgG) goat antibody (Vector) in PBS-XCD and then for 1 h with ABC. The bound peroxidase was developed brown by incubation for 30–60 min with DAB reaction mixture as described above.

Reconstruction and Morphological Analysis of Single VA-VL Neurons

The cell body, dendrites, and projecting axons of stained VA-VL neurons were reconstructed under a microscope attached with camera lucida apparatus. After the reconstructed figures were captured by a digital scanner, they were retraced and digitized in a computer with software CANVAS X (ACD Systems International Inc., Victoria, Canada). The axon fibers were reconstructed section by section onto a parasagittal plane and superimposed in the computer. The fine morphological indices, such as the width of axon varicosities or fibers, were measured with 100× objective lens (SPlanApo100; numerical aperture = 1.35; Olympus, Tokyo, Japan) and Neurolucida (MicroBright Field, Inc., Williston, VT), which was attached to light microscope Vanox (Olympus). The cytoarchitectonic areas and layer structures of cerebral cortex were determined after Nissl staining according to Paxinos and Watson (2007). For statistical analysis, such as Bonferroni post hoc multiple comparison test following 1-way analysis of variance and Student's *t*-test, software GraphPad Prism (Graphpad Software Inc., San Diego, CA) was used.

Results

Subdivision of VA-VL Complex

Before starting the single-cell tracing of motor thalamic neurons, we tried to subdivide the VA-VL motor thalamic complex into the 2 compartments that mainly receive the basal ganglia and cerebellar afferents. However, a distinction between the rat VA and VL is difficult to make in cytoarchitecture as described by Jones (2007) because the VA and VL are similarly cell sparse with relatively large neurons (Fig. 1*A, B*). On the other hand, some chemoarchitectonic structures were useful in dividing the VA-VL complex into 2 portions (Fig. 1*C-H*). Neuronal cell bodies and neuropil displayed much more immunoreactivity for calbindin D28k in the rostromedial portion than the caudolateral portion of the VA-VL complex (Fig. 1*C, D*), as shown previously (Paxinos et al. 1999; Bodor et al. 2008). In the present study, it was further observed that immunoreactivity for GAD67, a γ -aminobutyric acid (GABA)ergic marker, was also more intense in neuropil of the rostromedial portion than of the caudolateral portion of the VA-VL complex (Fig. 1*E, F*). Inversely, neuropil immunoreactivity for VGLuT2 was more abundant in the caudolateral portion but sparse in the rostromedial portion of the VA-VL complex (Fig. 1*G, H*). VGLuT2 is known to be a glutamatergic axon terminal marker, which is little expressed by telencephalic neurons but mainly produced by neurons in diencephalic and lower brain stem regions, including cerebellar nuclei (Freneau et al. 2001; Fujiyama et al. 2001; Herzog et al. 2001; Hioki et al. 2003). The distributions of GAD67 and VGLuT2 immunoreactivities were mostly complementary throughout the VA-VL complex. These results indicate that the rostromedial portion of the VA-VL complex receives abundant inhibitory afferents, probably derived

from the basal ganglia output nuclei, whereas the caudolateral portion admits excitatory subcortical afferents most likely from the cerebellar nuclei. Thus, in the following experiments, we divided the VA-VL complex into rostromedial and caudolateral portions, that is, inhibitory afferent-dominant zone (IZ) and excitatory subcortical afferent-dominant zone (EZ), respectively, applying immunofluorescence labeling for GAD67.

Selection of palGFP-Labeled Neurons for Single-Cell Tracing

Because almost all motor thalamic neurons projected to ipsilateral hemispheres (Donoghue and Parham 1983), palGFP-expressing Sindbis viral vector was injected into both hemispheres of 49 rat brains (thus 98 hemispheres). The survival time was as short as possible, that is, 50–55 h, to avoid possible effects of palGFP on the axonal morphology of the infected neurons. Of 98 virus-injected hemispheres, 37, 13, and 7 hemispheres (57 hemispheres in total) contained only 1, 2, and 3 of palGFP-expressing neurons, respectively. The remaining 41 hemispheres containing no or more than 3 palGFP-labeled neurons were not processed further because cortical axonal arborizations of more than 3 palGFP-positive thalamic neurons were almost always entangled with one another.

Subsequently, the localization of palGFP-labeled neurons in the 57 hemispheres was examined by immunofluorescent labeling for GAD67 and further confirmed in cytoarchitecture by counterstaining of propidium iodide. For example, in Figure 2*A', B*, a palGFP-positive neuron was identified as an IZ neuron because it was located in an intensely GAD67-immunoreactive region of the VA-VL complex. Although 84 neurons were found in the 57 hemispheres, only 38 VA-VL

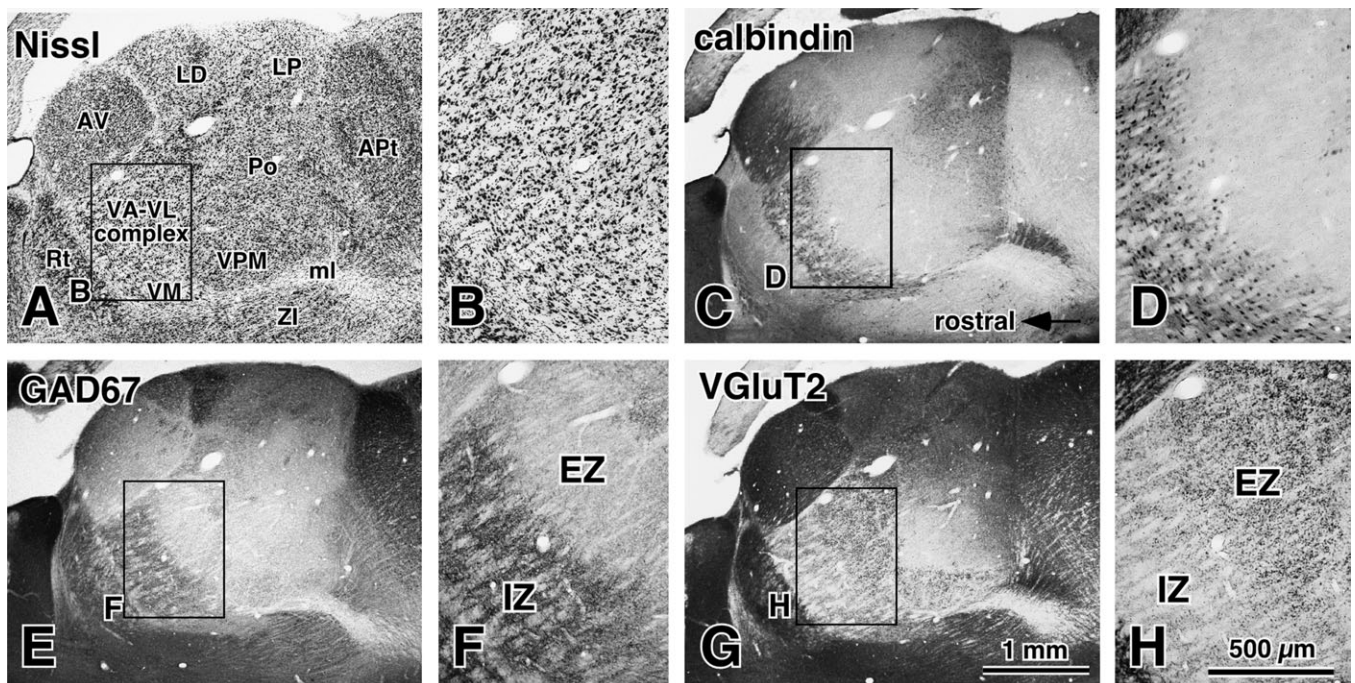


Figure 1. Cytoarchitecture and immunoreactivities for calbindin D28k, GAD67, and VGLuT2 in rat VA-VL complex. Although the cytoarchitecture of the VA-VL complex was homogeneous (*A, B*), some immunoreactivities showed heterogeneity in the complex. Immunoreactivities for calbindin (*C, D*) and GAD67 (*E, F*) were intense in the rostral portion but weak in the caudal portion of the VA-VL complex. In contrast, immunoreactivity for VGLuT2 (*G, H*) was more intense in the caudal portion than in the rostral portion. Images (*A, C, E, G*) were taken from the consecutive parasagittal sections. APT, anterior pretectal nucleus; AV, anteroventral thalamic nucleus; EZ, excitatory subcortical afferent-dominant zone; IZ, inhibitory afferent-dominant zone; LD, laterodorsal thalamic nucleus; LP, lateral posterior thalamic nucleus; ml, medial lemniscus; Po, posterior thalamic nuclear group; Rt, reticular thalamic nucleus; VM, ventromedial thalamic nucleus; VPM, ventral posteromedial thalamic nucleus; ZI, zona incerta. Scale bar in (*G*) applies to (*A, C, E, G*) and that in (*H*) to (*B, D, F, H*).

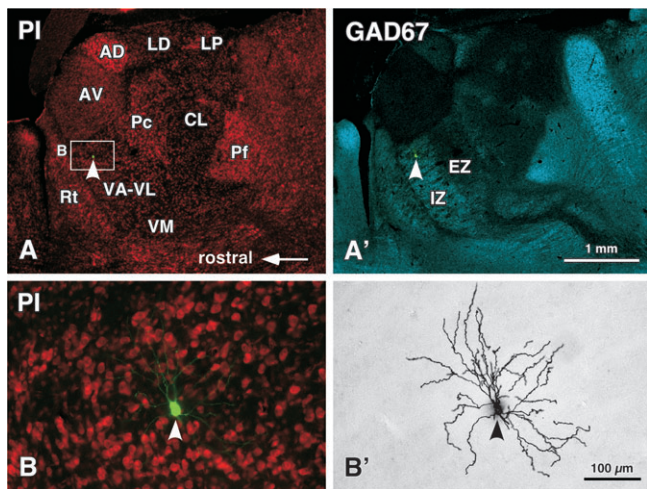


Figure 2. Classification of motor thalamic neurons infected with palGFP-Sindbis viral vector into EZ or IZ neurons. The sections that contained palGFP-labeled neuronal cell bodies (arrowheads; excitation, 488 or 450–490 nm; emission, 505–530 nm under the confocal laser-scanning or fluorescent microscope) were stained with propidium iodide (PI; *A, B*; excitation, 530–585 nm; emission, \geq 615 nm) and immunostained for GAD67 (Alexa Fluor 647; *A'*; excitation, 633 nm; emission, \geq 650 nm). After classifying motor thalamic neurons into EZ or IZ neurons, the labeled neurons were visualized by immunoperoxidase staining with the anti-GFP antibody (*B'*). AD, anterodorsal thalamic nucleus; CL, centrolateral thalamic nucleus; ml, medial lemniscus; Pc, paracentral thalamic nucleus; Pf, parafascicular thalamic nucleus; The other abbreviations, see the legend of Figure 1. Scale bar in (*A'*) applies to (*A, A'*) and that in (*B'*) applies to (*B, B'*).

neurons in 29 hemispheres were selected by excluding the neurons that were located outside of the VA-VL complex or on the border between the VA-VL complex and the surrounding nuclei. These selected neurons were composed of 22 IZ neurons and 16 EZ neurons.

The sections of the 29 hemispheres were then processed for GFP immunoperoxidase staining by the ABC method with the BT-GO amplification (Figs 2*B'* and 5). Twenty of the 22 IZ neurons mainly sent axons to the primary and secondary motor areas, and 14 of the 16 EZ neurons chiefly projected to the motor areas. The remaining 2 IZ neurons did not project to the motor areas, but to the posterior parietal area, being excluded from the present analysis. Although the remaining 2 EZ neurons sent some axons to the primary motor area, the main target of these EZ neurons was the lateral orbital area. Because the present study was focused on the thalamocortical projections that were mainly targeted to the motor areas, we also excluded these 2 EZ neurons from the present analysis. Subsequently, 15 of the 20 IZ neurons and 9 of the 14 EZ neurons were removed from the analysis, mainly because their cortical axonal arborization was entangled with that of the other coinfecting thalamic neurons. Thus, only 5 IZ neurons and 5 EZ neurons, the axonal arborization of which could be completely isolated, were selected for further morphological analysis, as shown in Table 1. The location of their cell bodies in the VA-VL complex was plotted onto the parasagittal plane in Figure 3.

Cell Bodies and Dendrites of IZ and EZ Neurons

Both the reconstructed IZ and EZ neurons were multipolar neurons with many dendrites (Fig. 2*B'*) as reported previously in rat thalamus (Sawyer et al. 1989, 1994; Yamamoto et al. 1991). When the dendrites were reconstructed and projected to a sagittal plane (Fig. 4*A, B*), it was noticed that the dendrites of

Table 1

Thalamic neurons analyzed in the present study

Neuron	Total number of labeled neurons in a hemisphere	Location of other neurons in the thalamus	Target fields in cortical areas	Axon bush in the striatum
IZ				
1	2	IZ ^a	M1, M2, HL, S1	+
2	1	—	M1, M2, FL, HL, S1	+
3	1	—	M1, HL, FL, S1	+
4	2	AV	M1, M2, FL, S1, FrA	+
5	1	—	M1, M2, HL, S1, Cg	+
EZ				
6 ^b	3	EZ, VPM	M1, FL, S1	— ^c
7 ^b	3	EZ, VPM	M1, S1	— ^c
8	2	VPL	M1, M2, HL, S1	—
9	1	—	M1, M2, FL, S1, FrA	—
10	1	—	M1, FL	—

Note: AV, anteroventral nucleus; Cg, cingulate area; FL, forelimb area; FrA, frontal association area; HL, hindlimb area; M1, primary motor area; M2, secondary motor area; S1, primary somatosensory area excluding FL and HL areas; VPL, ventral posterolateral nucleus; VPM, ventral posteromedial nucleus.

^aThis IZ neuron did not project to motor areas but to parietal association areas and was thus excluded from the present analysis.

^bThese 2 EZ neurons were found in a hemisphere of a rat, but their axonal arborization was fortunately separable. Furthermore, this hemisphere contained another VPM neuron, the axonal arborization of which was also separable from that of the EZ neurons.

^cNeurons 6 and 7 had a tiny short axon collateral in the neostriatum but never made an axon bush in the striatum.

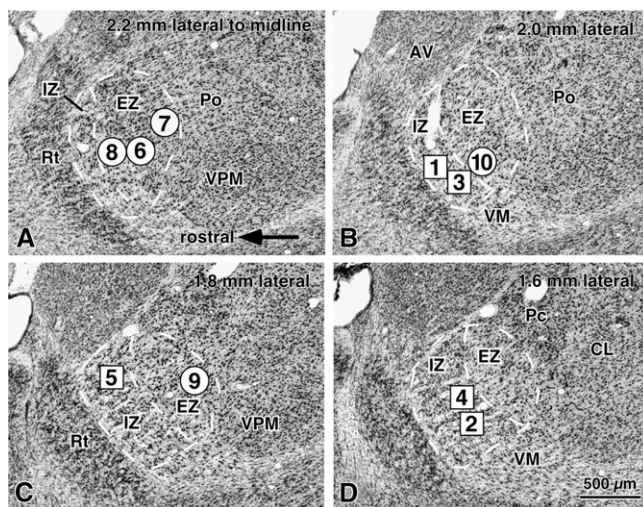


Figure 3. The location of motor thalamic neurons analyzed in the present study. Neurons 1–5 in the IZ and neurons 6–10 in the EZ were projected onto the nearest sagittal plane of Nissl-stained sections. The white broken lines between the IZ and EZ were determined on the basis of GAD67 immunoreactivity in the adjacent sections. Abbreviations, see the legends of Figures 1 and 2. Scale bar in (*D*) applies to (*A–D*).

IZ neurons were fewer than those of EZ neurons. We quantitatively confirmed this result using the Sholl analysis (Sholl 1953); the number of dendritic intersections of IZ neurons was significantly smaller at circles of 60–120 μ m apart from the cell body compared with that of EZ neurons (Fig. 4*C*). This may reflect the functional difference of EZ and IZ neurons, which receive excitatory and inhibitory afferents, respectively, as a main input source. In contrast, the extent of dendritic processes was not significantly different between IZ and EZ neurons.

The region around each palGFP-positive neuronal cell body was darkly immunostained (Fig. 2*B'*) probably because of extracellularly leaked palGFP, suggesting an extremely strong expression of protein by the subgenomic promoter of Sindbis

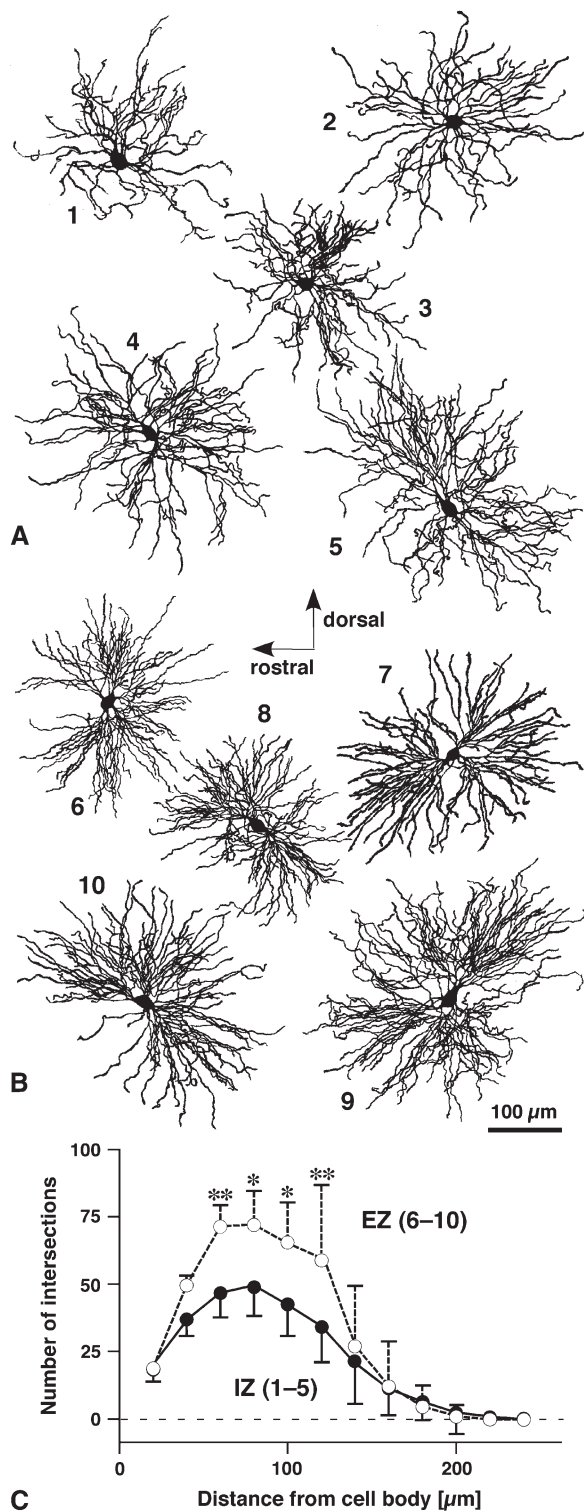


Figure 4. Dendrites and cell bodies of motor thalamic neurons. IZ neurons (1–5; *A*) had much less dendritic processes than EZ neurons (6–10; *B*). The Sholl analysis revealed that the difference was statistically significant at distances of 60–120 μm from the cell body (*C*; $*P < 0.05$, $**P < 0.01$, Bonferroni multiple comparison test). The filled circles and open circles in (*C*) indicate the data of IZ neurons and EZ neurons, respectively, and the data are shown as mean \pm SD. Scale bar in (*B*) applies to (*A* and *B*).

viral vector. However, neither spread of palGFP to nor uptake by adjacent cell bodies was found. Although the measurement of the cell bodies was inaccurate, we observed no significant

difference ($P = 0.81$ by the 2-tailed unpaired *t*-test) between the areas of IZ and EZ neuronal cell bodies, which were 245 ± 21 and $250 \pm 25 \mu\text{m}^2$ (mean \pm standard deviation [SD]), respectively.

Axonal Arborization of IZ and EZ Neurons

The axonal arborization of single motor thalamic neurons was almost completely reconstructed as shown in Figures 6–8. Every axon fiber (Fig. 5*A, C*) was clearly labeled, and axon varicosities were easily detectable (Fig. 5*B, D*) by the combination of the ABC method with the BT-GO amplification. No motor thalamic neurons reconstructed in the present study possessed axon collaterals inside of the VA-VL complex. When the axons exited from the thalamus, both the IZ and EZ neurons always emitted axon collaterals to the thalamic reticular nucleus (open arrowheads in Fig. 5*E*). The largest difference in subcortical regions between IZ and EZ neurons was the presence and absence of a striatal axon collateral bush, respectively (Table 1 and Figs 5*F* and 6–8; Supplementary Figs 1 and 2). No or few axon collaterals to the striatum were observed in the EZ neurons (Table 1). This result was confirmed in the other 24 motor area-projecting VA-VL neurons, which were not reconstructed because of the overlapping axonal arborization with other neurons (Table 3). As far as we could determine (4 of 9 EZ neurons and 11 of 15 IZ neurons), no EZ neurons formed intrastriatal axon bushes, and all the IZ neurons formed rich bushes.

In the cerebral cortex, both the reconstructed IZ and EZ neurons sent axon fibers to widespread areas including the primary and secondary motor areas (M1 and M2 in Table 1; for the detail of cortical area identification, see Supplementary Fig. 1). Some neurons also projected to the primary somatosensory, forelimb, hindlimb, cingulate, and frontal association areas. Because forelimb and hindlimb areas were reported to share the electrophysiological characteristics of the primary motor area (Hall and Lindholm 1974; Donoghue and Wise 1982), it is comprehensible that IZ and EZ neurons projected to these areas. Unexpectedly, not only the IZ neurons but also 4 of the 5 EZ neurons reconstructed sent axons to the primary somatosensory area (Table 1; Figs 6–8; Supplementary Figs 1 and 2). Moreover, the cortical axonal arborization showed a tendency to make several bushes in 3 of the 5 IZ neurons (Figs 6*A* and 7*A, C*) and only 1 of the 5 EZ neurons (Supplementary Fig. 2*E*).

Furthermore, the largest difference in cortical arborization between IZ and EZ neurons was found in their laminar preference. As shown in Figures 6–8, the axon fibers of IZ neurons were most abundantly distributed in layer I, whereas those of EZ neurons were mainly located in layers II–V with little arborization in layer I. Although layer I axon fibers appeared to be mixed with layers II–VI fibers in Figures 7*B* and 8*B*, the mixture was caused by the projection of those fibers to a parasagittal plane, which was near the tangential plane to the lateral cortical areas. The differential laminar preference of VA-VL neurons was reproducible in all the IZ and EZ neurons (Table 2). As axon varicosities were important sites for synaptic transmission, the number of axon varicosities in each layer was estimated by multiplying the length of varicose axon fibers with the mean density of varicosities in the layer (see Supplementary Table). In cortical axon fibers of the 5 IZ neurons, 47–66% of the varicosities were estimated to be distributed in layer I (Table 2), especially in the upper part of layer I (Fig. 5*A*). It was also noticed that some IZ neurons, for example, neuron 5 (Fig. 7*C–F*), showed

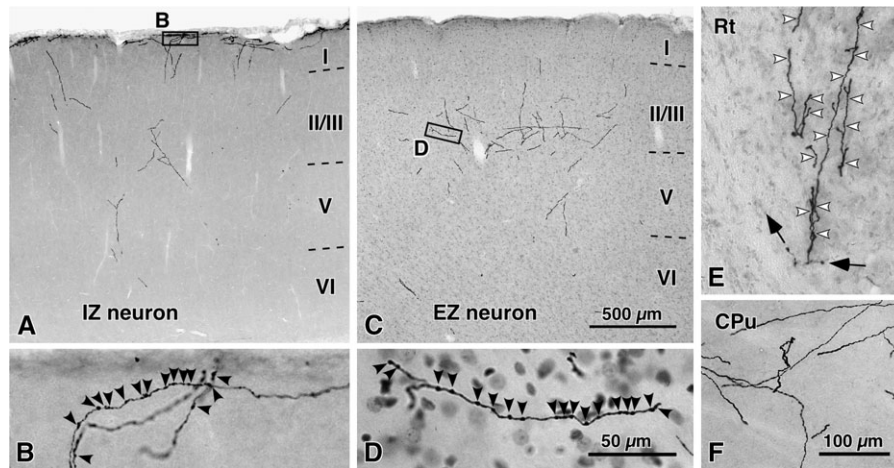


Figure 5. Axon fibers and varicosities of motor thalamic neurons. Axon fibers of IZ neurons were distributed in the superficial portion of motor areas (A, B) and neostriatum (CPu; F), whereas those of EZ neurons were in the deep portion of layer II/III of motor areas (C, D). Both IZ and EZ neurons had axon collaterals in the thalamic reticular nucleus (Rt; open arrowheads in E). Arrows in (E) indicate the main axons, which were more lightly labeled than collaterals probably because of the myelination. Filled arrowheads in (B and D) indicate axon varicosities that were located at a focus plane of the microscope. To determine cortical areas and layers, we counterstained sections for Nissl with cresyl violet after the reconstruction (C, D, E). The counterstaining was not clear in (C and E) because the cresyl violet color was photographically suppressed with 450-nm-centered band-pass filter, but clear in (D) using the usual 550-nm band-pass filter. Scale bar in (C) applies to (A and C), that in (D) applies to (B and D), and that in (F) applies to (E and F).

various axonal preferences for layer I in different axon bushes (compare Fig. 7D with E, F). In contrast, only 2–15% of axon varicosities of the 5 EZ neurons were located in layer I of the cortical areas. Although neuron 9, of the 5 EZ neurons, had the most abundant axonal arborization in layer I, the main cortical axon bush of neuron 9 was located in layers II–V (Fig. 8B). This finding of the reconstructed neurons was supported by the observation in the 24 VA–VL neurons without reconstruction, as far as we could determine (Table 3; 7 of 9 EZ neurons and 11 of 15 IZ neurons). Thus, the conclusion on the axonal arborization indicates that IZ neurons are clearly distinct from EZ neurons in terms of the targets to which their information should be transferred.

Control Experiments with GFP-Sindbis Viral Vector

Overexpression of palGFP was recently reported to induce filopodia formation on the surface membrane of cultured COS-7 cells and on the dendrites of cultured hippocampal neurons (Gauthier-Campbell et al. 2004). In the present study, no growth cone- or filopodia-like formation was found in the axonal or dendritic processes of the thalamic neurons infected in vivo with palGFP-Sindbis virus. However, it is possible that palGFP expression might have affected the axonal arborization of thalamic neurons. Thus, we compared axon fibers of palGFP-Sindbis virus-infected thalamic neurons with those of GFP-labeled thalamic neurons using some morphological indices.

We injected a relatively high concentration of GFP-Sindbis viruses into the VA–VL complex, and it took a longer survival time of 72–96 h to visualize cortical axon fibers as clearly as possible. Because some axon fibers of VA–VL neurons infected with GFP-Sindbis virus were not completely labeled, we randomly selected the seemingly well-stained axon fibers in the cerebral cortex and compared them with palGFP-labeled axon fibers. The varicosity densities along palGFP- and GFP-labeled axon fibers in motor cortical areas were $112 \pm 18/\text{mm}$ (mean \pm SD; $n = 918$; data from Supplementary Table) and $115 \pm 18/\text{mm}$ ($n = 50$), respectively. The size of varicosities and the thickness of intervaricosity axon fibers were 1.70 ± 0.33 and $0.91 \pm 0.053 \mu\text{m}$ ($n = 100$ and 50) in palGFP-labeled axon fibers

and 1.74 ± 0.38 and $0.89 \pm 0.076 \mu\text{m}$ ($n = 100$ and 50) in GFP-labeled ones. No statistically significant differences in these morphological indices were detected between palGFP-positive and GFP-positive axon fibers ($P \geq 0.38$ by the 2-tailed unpaired *t*-test). Thus, in the limit of the present control study, we concluded that the axonal morphology was little, if any at all, affected by the addition of palmitoylation signal.

Discussion

Two types of thalamocortical projections were found in rat motor thalamic nuclei by using the single neuron-tracing method with the palGFP-Sindbis viral vector (Fig. 9A). Motor area-projecting VA–VL neurons were divided into IZ and EZ neurons based on GABAergic and glutamatergic terminal markers. All the IZ neurons examined sent axon fibers not only to cortical areas but also to the neostriatum, whereas all the EZ neurons selectively projected to cortical areas. The main cortical target of EZ neurons was layers II–V and that of IZ neurons was layer I. Thus, motor thalamic nuclei were revealed to contain 2 distinct kinds of thalamocortical projection neurons.

Technical Considerations

As described in Results, the effect of adding palmitoylation signal to GFP was considered to be minimal, if at all, on the axonal morphology of the infected neurons in adult rats. Similar results in adult rats were observed with the GFP attached with the fatty acylation signal, myristoylation, and palmitoylation signal, of Fyn (Kameda et al. 2008). The expression of fatty acylation site-attached GFP produced no filopodia-like or growth cone-like changes in neuronal processes and had little effect on the morphological indices of the dendrites, such as the length of spine necks, the size of spines, and the width of dendrites, in cortical pyramidal neurons and medium-sized spiny neostriatal neurons. Thus, in general, it seems unlikely that the attachment of a fatty acylation site to GFP affects the morphology of mature neurons.

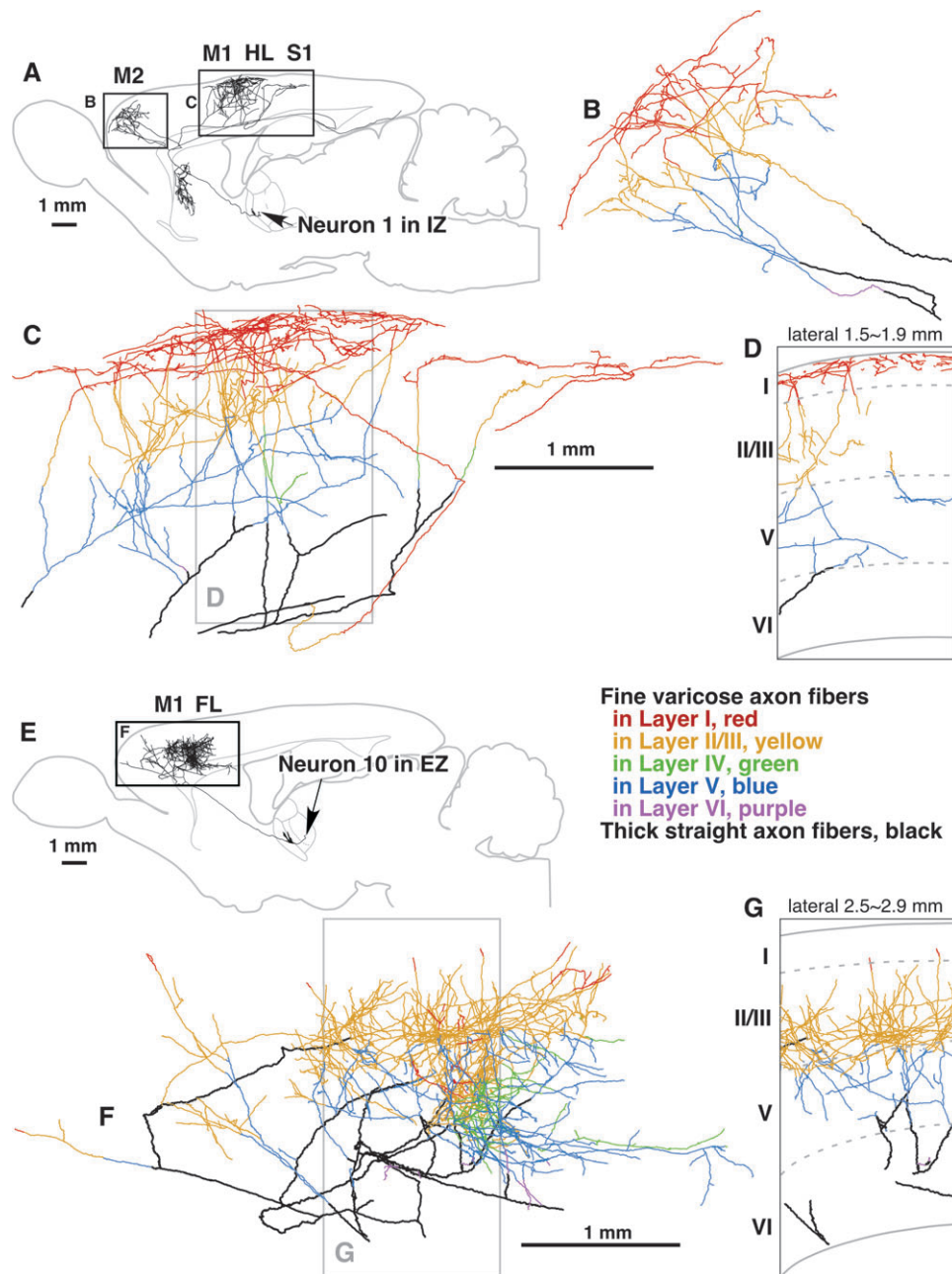


Figure 6. Camera lucida reconstruction of 2 motor thalamocortical axons. Axon fibers of IZ neurons were widely distributed in motor-associated areas and neostriatum (A). Of cerebral cortical layers, layer I was most intensely innervated by the axon fibers of IZ neurons (B–D). In contrast, axon fibers of EZ neurons were found only in motor-associated areas (E) and distributed mainly in cortical layers II–V (F, G). Figures (D and G) are representative planes, in which the results of serial 10 sections were superimposed onto a parasagittal plane of the fifth section. FL, forelimb region of primary somatosensory-motor area; HL, hindlimb region of primary somatosensory-motor area; M1, primary motor area; M2, secondary motor area; S1, primary somatosensory area.

The distribution of cortical axons of VA–VL neurons in the present study was included in the cortical areas and layers that were reported to receive inputs from the rat VA–VL complex (Donoghue et al. 1979; Cicirata et al. 1986; Yamamoto et al. 1990; Aumann et al. 1998; Wang and Kurata 1998; Mitchell and Cauller 2001). Furthermore, in a preliminary study where a palGFP–Sindbis virus solution of a high titer was injected into the rat VA–VL, numerous VA–VL neurons were labeled with palGFP (data not shown), and the distribution of their palGFP-labeled axon fibers was almost the same as the previously reported one in the rat cerebral cortex and striatum

(Yamamoto et al. 1990; Cheatwood et al. 2005). These results indicate that VA–VL neurons are nonselectively infected with the Sindbis viral vector.

Two Types of Thalamocortical Projections of the VA–VL Complex

In the present study, the rat VA–VL complex was segregated into 2 compartments, rostromedially located IZ and caudolaterally placed EZ on the basis of the differential immunoreactivities for GAD67 and VGluT2. The VA–VL complex is known to receive GABAergic afferents not only from the basal ganglia but also from

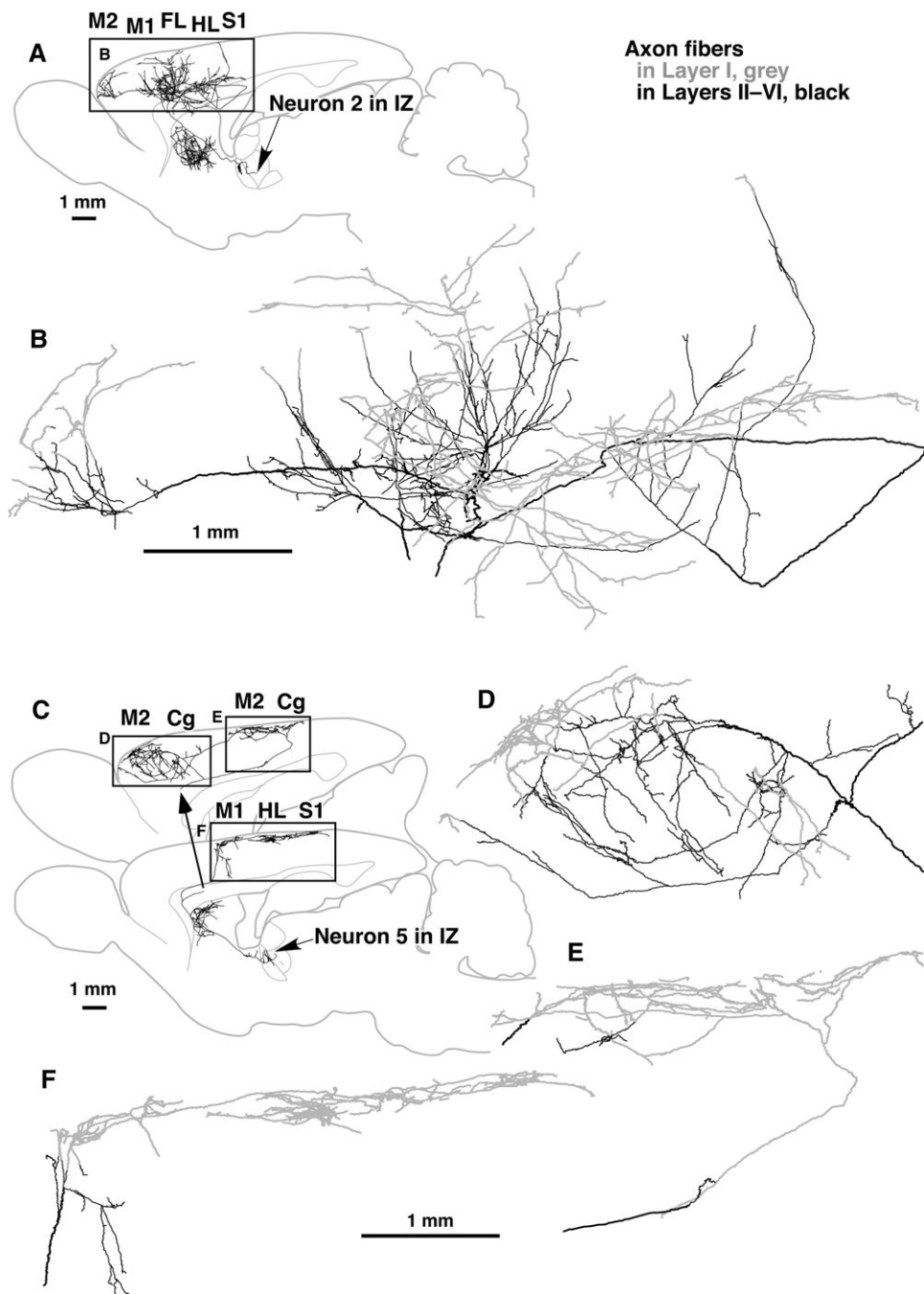


Figure 7. Axonal arborization of 2 IZ neurons. Axon fibers of IZ neurons were widely observed in motor-associated areas and neostriatum (A, C) and densely distributed in layer I of those cortical areas (gray lines in B, D–F). Cg, cingulate area; The other abbreviations, see the legend of Figure 6.

the thalamic reticular nucleus. Because parvalbumin-immunoreactive fibers, which are mainly emitted from thalamic reticular nucleus neurons, are distributed rather homogeneously in the VA-VL complex (Paxinos et al. 1999), the thalamic reticular nucleus is considered to evenly project to the VA-VL complex. Thus, the difference in GAD67 immunoreactivity between the IZ and EZ may reflect the fact that the basal ganglia afferents are principally distributed in the IZ. On the other hand, main glutamatergic afferents to the VA-VL complex are derived from the cerebral cortex and deep cerebellar nuclei, and these 2 afferents have fortunately been differentiated with VGluT1 and VGluT2 immunoreactivities, respectively (for review, cf., Kaneko

and Fujiyama 2002). Thus, the chief target of the cerebellar afferents may be the EZ with intense VGluT2-immunoreactive neuropil. Finally, this IZ-EZ segregation of the VA-VL complex is supported by the distributions of basal ganglia and cerebellar afferents, which were rostromedially and caudolaterally located in the rat VA-VL complex, respectively (Carter and Fibiger 1978; Faull and Carman 1978; Angaut et al. 1985; Deniau et al. 1992; Aumann et al. 1996; Sakai et al. 1998; Bodor et al. 2008).

Recently, it has been proposed that primate thalamic nuclei are divided into the core and matrix nuclei by the dominance of parvalbumin- and calbindin-producing neurons, respectively (for review, see Jones 1998, 2001). Intensely

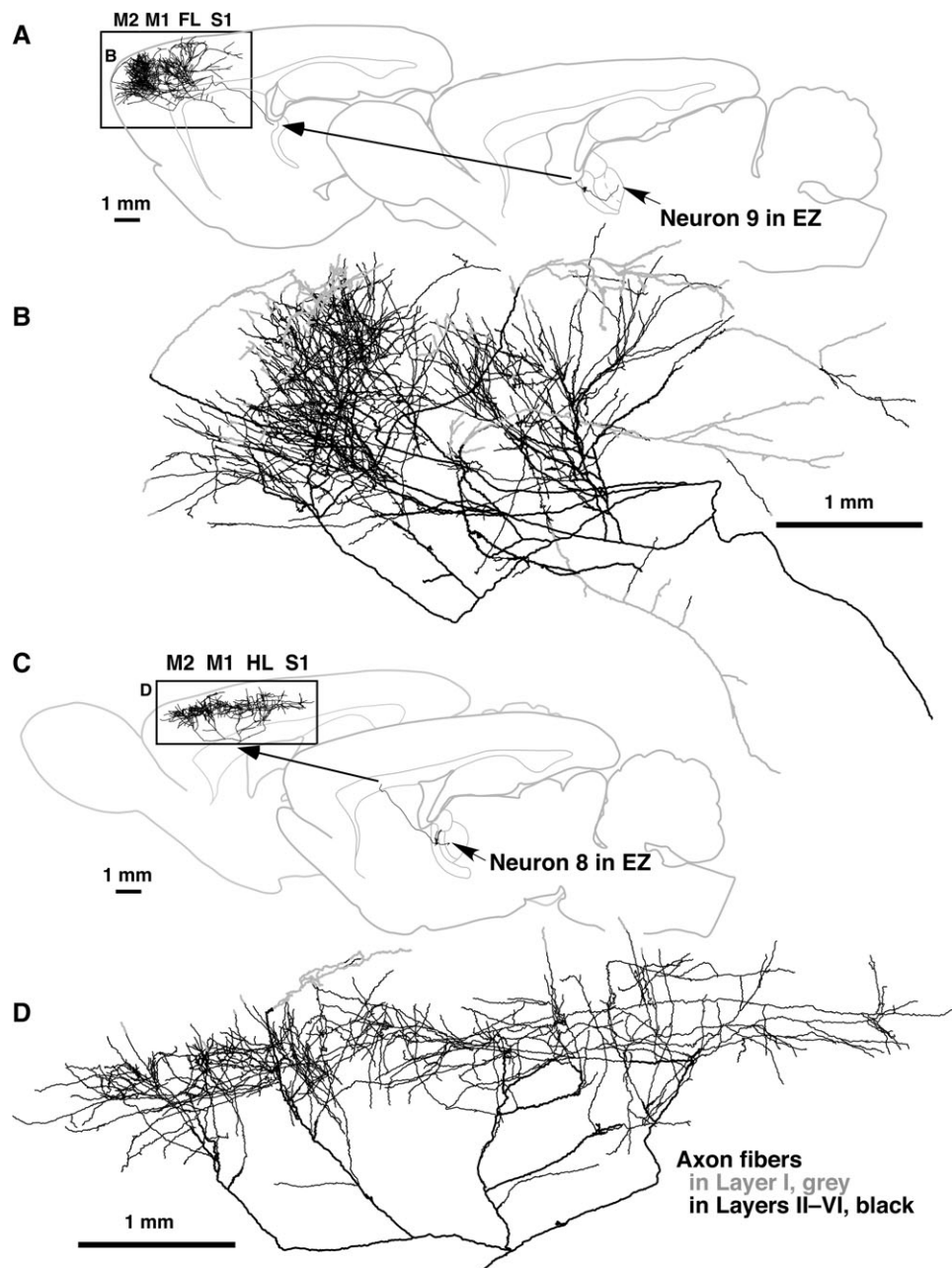


Figure 8. Axonal arborization of 2 EZ neurons. Axon fibers of EZ neurons were essentially localized to motor-associated areas (A, C), where the fibers were distributed mainly in layers II–V of those areas (black lines in B, D). Of the 5 EZ neurons, neuron 9 sent the most abundant axon fibers to layer I (about 15% of total axon fibers; gray lines in B) and neuron 8 showed most widespread distribution of axon fibers in the cerebral cortex (about 5 mm; D). Abbreviations, see the legend of Figure 6.

parvalbumin-immunoreactive neurons were distributed in the VLc, and strongly calbindin-positive neurons were located in VA/VLo of the monkey thalamus. Although no parvalbumin-immunoreactive neurons were found in the rat thalamic nuclei except the reticular nucleus, many IZ but no EZ neurons expressed calbindin immunoreactivity (Paxinos et al. 1999; Bodor et al. 2008; Fig. 1D). In addition, in the core-matrix concept of the thalamic nuclei, matrix neurons project to the superficial layers of the cerebral cortex over relatively wide areas, whereas core neurons project to the middle layers of the cortex in an area-specific manner (Jones 1998, 2001). This concept is in a good agreement with the present results that IZ neurons sent $54 \pm 5\%$ of their axons to layer I of relatively wide areas.

The 2 types of thalamocortical projections in motor areas have been suggested in early electrophysiological works. Sasaki et al. (1970) reported that electrical stimulation of cat VA-VL complex evoked an early excitatory postsynaptic potential (EPSP) response in the deep layers of cat primary motor area, followed by a late EPSP in the superficial layer. Later, not only early deep responses but also late superficial responses in the primary motor area were evoked by cerebellar nucleus stimulation in cats (Sasaki et al. 1972) and monkeys (Sasaki et al. 1976; Sasaki and Gemba 1981, 1982). More recently, most VA-VL neurons, which were inhibited by stimulation of the internal segment of the globus pallidus, were activated by the antidromic stimulation in layer I of the primary motor area

Table 2

Axonal arborization of motor thalamic neurons in the cerebral cortical areas

Neuron	Total axon length in cortex (μm) ^a	Estimated number of varicosities in cortex ^b	Axon length in layer I (μm) ^a	Estimated number of varicosities in layer I ^b
IZ				
1	175246	19681	80838 (46.1%)	9215 (46.8%)
2	186336	20545	96765 (51.9%)	10644 (51.8%)
3	181606	20240	97666 (53.8%)	10939 (54.0%)
4	290706	33143	146159 (50.3%)	16954 (51.2%)
5	197204	22486	129431 (65.6%)	14885 (66.2%)
Mean \pm SD	206220 \pm 33795	23219 \pm 3970	110172 (53.5%) \pm 22099 (\pm 4.9%)	12527 (54.0%) \pm 2714 (\pm 4.9%)
EZ				
6	131261	14594	7566 (5.8%)	870 (6.0%)
7	217210	23992	6153 (2.8%)	689 (2.9%)
8	214979	24903	5254 (2.4%)	599 (2.4%)
9	385131	42069	55022 (14.3%)	6162 (14.6%)
10	221815	25357	6374 (2.9%)	733 (2.9%)
Mean \pm SD	234079 \pm 60421	26183 \pm 6354	16074 (5.6%) \pm 15579 (\pm 3.5%)	1811 (5.8%) \pm 1741 (\pm 3.6%)

^aThe length of axon fibers was estimated by multiplying the length of varicose axons projected onto parasagittal plane by $\pi/2$. Thus, the measured axons did not contain thick straight axon fibers, which might be myelinated portions of thalamocortical axons and make no synaptic contacts.

^bThe estimated number of varicosities in each cortical layer was calculated by multiplying, in each layer, axon length by the density of varicosities. The mean density of varicosities was, in each layer, measured with 20 randomly selected axon fibers, which were longer than 100 μm . See Supplementary Table for the original data.

(Jinnai et al. 1987). These results suggested the presence of at least 2 types of VA-VL neurons; one fast-conducting type of cerebellar afferent-receiving neurons in the VA-VL complex sent their axons only to deep cortical layers, whereas the other slow-conducting type of cerebellar and/or pallidal afferent-admitting neurons projected to layer I. The present study supported the presence of 2 types of deep and superficial thalamocortical projections of VA-VL neurons. However, all the reconstructed EZ neurons, probably transmitting cerebellar information, almost selectively projected to the deep cortical layers. If only EZ neurons convey cerebellar information to rat motor areas, the present findings are not in agreement with the previous results on cerebellar afferent-receiving VA-VL neurons of cat and monkey. This discrepancy will be solved by future single neuron-tracing studies of cat and monkey VA-VL neurons, although it might be accounted for by the species difference.

Functional Implication of IZ and EZ Neurons in the Motor Systems

Apart from cortical axonal arborization, we have noticed another important difference in thalamostriatal projection between IZ and EZ neurons. The striatal projection of VA-VL neurons has been reported in the primate brain, in which VLo and VA neurons send many axons and VLc and ventral posterolateral pars oralis nucleus neurons less extensively project to the dorsal striatum (McFarland and Haber 2000, 2001). Furthermore, recently, Hoshi et al. (2005), using the transsynaptic retrograde tracing technique with the rabies virus, reported that some cerebellar dentate nucleus neurons were trisynaptically connected to the external pallidum via the thalamus and striatum. However, to our surprise, no EZ neurons formed axon collateral bushes in the neostriatum (Fig. 9A), although IZ neurons sent massive axon collaterals to the neostriatum like the monkey motor thalamic nuclei. Therefore, in terms of thalamostriatal projection, EZ neurons, which probably received cerebellar afferents, were seemingly segregated from the basal ganglia system at least in the rat brain. In contrast, as the IZ is considered to receive massive basal ganglia afferents, this thalamostriatal projection appears to be a feedback projection, like the thalamostriatal projection of intralaminar thalamic nuclei, which are well known to

Table 3

Axonal distribution of the 24 motor area-projecting VA-VL neurons, which were not reconstructed, in the cerebral cortex and striatum

	Total number	Arborization in cortical layer I			Axon bush formation in the striatum		
		Rich	Poor	nd ^a	Present	Absent	nd ^b
IZ neuron	15	11	0	4	11	0	4
EZ neuron	9	0	7	2	0	4	5

^aNot determined. Each of 4 IZ neurons was costained with EZ neurons or ventral medial (VM) nucleus neuron, and each of 2 EZ neurons with IZ neurons in the same hemisphere. Because the axonal arborization of IZ or EZ neurons was intermingled with that of the costained EZ/VM or IZ neurons, respectively, in cortical layers, it was difficult to determine whether these IZ or EZ neurons had rich axonal arborization in layer I or not.

^bEach of 4 IZ neurons was colabeled with EZ or VM neurons, and each of 5 EZ neurons with IZ or paracentral nucleus neurons in the same hemisphere. Because of the overlapping axonal distribution in the striatum, the axon bush formation of these IZ and EZ neurons was not determined.

receive basal ganglia afferents (for review, cf., Groenewegen and Witter 2004; Jones 2007).

When compared with the single axonal arborization of rat sensory thalamocortical neurons (Jensen and Killackey 1987; Arnold et al. 2001; Oda et al. 2004), the axonal arborization of EZ and IZ neurons was more widespread and extended more than 2 mm in the rostrocaudal direction (Figs 6–8; Supplementary Figs 1 and 2). They were distributed not only in the primary and secondary motor areas but also in the primary somatosensory areas including the forelimb and hindlimb areas (S1, FL, and HL in Table 1). From the viewpoint of the core-matrix organization (Jones 1998, 2001), the presumed core component of the motor thalamus, EZ neurons, seemed unique in the broadness of cortical arborization compared with core neurons in the sensory thalamus. Furthermore, because both the axon bushes of single EZ and IZ neurons were widely distributed in motor areas, it is highly likely that both the bushes should largely overlap with each other (Fig. 9A). In fact, in the course of the present experiment, when IZ and EZ neurons were coinfecting with the viral vectors in a hemisphere, the axonal arborizations of those IZ and EZ neurons were very frequently intermingled with each other in motor areas. Thus, pyramidal neurons of motor areas are considered to be simultaneously under the control of the 2 different types of thalamocortical afferents.

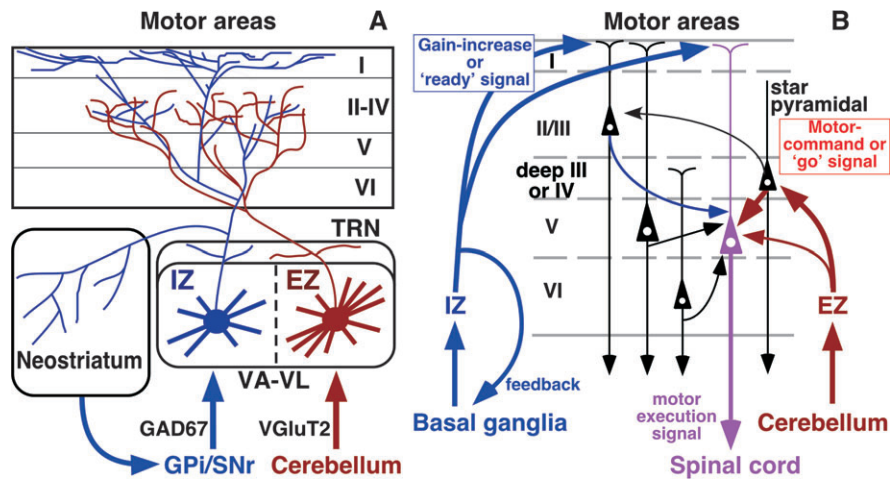


Figure 9. (A) Schematic diagram of motor thalamocortical projections. IZ neurons send axons not only to the cerebral cortex but also to the neostriatum, whereas EZ neurons selectively project to the cerebral cortex. Furthermore, the main cortical target of EZ neurons is layers II–V and that of IZ neurons includes layer I. GPI, internal segment of the globus pallidus; SNr, substantia nigra pars reticulata; TRN, thalamic reticular nucleus. (B) Function of EZ and IZ neurons in the context of motor execution. The drawing was modified from Figure 9 in Cho, Segawa, Okamoto et al. (2004), where intracortical inputs to layer V corticospinal neurons were revealed. See text for more details.

In our previous studies (Cho, Segawa, Mizuno, and Kaneko 2004; Cho, Segawa, Okamoto, et al. 2004), layer IV star-pyramidal neurons in motor areas including hindlimb-forelimb areas sent many axon fibers to layer V corticospinal neurons, and layer II/III pyramidal neurons less abundantly but significantly projected to the corticospinal neurons (Fig. 9B). Because the star-pyramidal neurons have poor apical dendrites, they may not preferentially receive layer I thalamocortical afferents from IZ neurons. Instead, the star-pyramidal neurons may principally receive middle layer afferents from EZ neurons transmitting cerebellar motor commands and transfer the commands to layer V corticospinal neurons. In contrast, as layer II/III and layer V pyramidal neurons have well-developed apical dendrites and tufts in layer I, their apical dendrites seem to be a main target of IZ axons conveying basal ganglia information. It has been indicated that layer I thalamocortical afferents are associated with the cortical activity prior to the motor execution (for review, cf., Roland 2002) and that layer I afferents modulate the gain of pyramidal cell response (Larkum et al. 2004). Thus, we may assume that the basal ganglia system produces motor preparatory information with its disinhibitory mechanism, and this information (gain-increase or “ready” signal in Fig. 9B) is conveyed via IZ neurons directly or through layer II/III pyramidal neurons to layer V corticospinal neurons in motor areas. We can further presume that, when the corticospinal neurons are prepared for the action by the gain-increase signal, the cerebellar motor command (motor-command or “go” signal in Fig. 9B), which is transferred via EZ neurons directly or through layer IV star-pyramidal neurons to corticospinal neurons, easily activates the corticospinal neurons to discharge the motor execution signal to the spinal cord. Even if this scheme is too much simplified and may not really work in the motor system, EZ and IZ neurons are sure to cooperate in producing an appropriate motor activity.

Funding

The Ministry of Education, Culture, Sports, Science and Technology Grants-in-Aid for Encouragement of Scientists (20-704 to EK); Young Scientists (20700316 to TF, 18700341 and 20700315 to HH, 19700317 to KN); Scientific Research

(16200025 and 17650100 to TK); Scientific Research on Priority Areas (17022020 to TK).

Supplementary Material

Supplementary material can be found at <http://www.cercor.oxfordjournals.org/>.

Notes

Conflict of Interest: None declared.

Address correspondence to email: kaneko@mbs.med.kyoto-u.ac.jp.

References

- Angaut P, Cicirata F, Serapide F. 1985. Topographic organization of the cerebellothalamic projections in the rat. An autoradiographic study. *Neuroscience*. 15:389–401.
- Arnold PB, Li CX, Waters RS. 2001. Thalamocortical arbors extend beyond single cortical barrels: an in vivo intracellular tracing study in rat. *Exp Brain Res*. 136:152–168.
- Asanuma H, Fernandez J. 1974. Characteristics of projections from the nucleus ventralis lateralis to the motor cortex in the cats: an anatomical and physiological study. *Exp Brain Res*. 20:315–330.
- Aumann TD, Ivanusic J, Horne MK. 1998. Arborization and termination of single motor thalamocortical axons in the rat. *J Comp Neurol*. 396:121–130.
- Aumann TD, Rawson JA, Pichitpornchai C, Horne MK. 1996. Projections from the cerebellar interposed and dorsal column nuclei to the thalamus in the rat: a double anterograde labelling study. *J Comp Neurol*. 368:608–619.
- Bodor L, Giber K, Rovo Z, Ulbert I, Acsady L. 2008. Structural correlates of efficient GABAergic transmission in the basal ganglia-thalamus pathway. *J Neurosci*. 28:3090–3102.
- Bredenbeek PJ, Frolov I, Rice CM, Schlesinger S. 1993. Sindbis virus expression vectors: packaging of RNA replicons by using defective helper RNAs. *J Virol*. 67:6439–6446.
- Carter DA, Fibiger HC. 1978. The projections of the entopeduncular nucleus and globus pallidus in rat as demonstrated by autoradiography and horseradish peroxidase histochemistry. *J Comp Neurol*. 177:113–124.
- Cheatwood JL, Corwin JV, Reep RL. 2005. Overlap and interdigitation of cortical and thalamic afferents to dorsocentral striatum in the rat. *Brain Res*. 1036:90–100.
- Cho R-H, Segawa S, Mizuno A, Kaneko T. 2004. Intracellularly labeled pyramidal neurons in the cortical areas projecting to the spinal

- cord—I. Electrophysiological properties of pyramidal neurons. *Neurosci Res.* 50:381-394.
- Cho R-H, Segawa S, Okamoto K, Mizuno A, Kaneko T. 2004. Intracellularly labeled pyramidal neurons in the cortical areas projecting to the spinal cord—II. Intra- and juxta-columnar projection of pyramidal neurons to corticospinal neurons. *Neurosci Res.* 50:395-410.
- Cicirata F, Angaut P, Cioni M, Serapide MF, Papale A. 1986. Functional organization of thalamic projections to the motor cortex. An anatomical and electrophysiological study in the rat. *Neuroscience.* 19:81-99.
- Deniau JM, Kita H, Kitai ST. 1992. Patterns of termination of cerebellar and basal ganglia efferents in the rat thalamus—strictly segregated and partly overlapping projections. *Neurosci Lett.* 144:202-206.
- Deschênes M, Hammond C. 1980. Physiological and morphological identification of ventrolateral fibers relaying cerebellar information to the cat motor cortex. *Neuroscience.* 5:1137-1141.
- Donoghue JP, Kerman KL, Ebner FF. 1979. Evidence for two organizational plans within the somatic sensory-motor cortex of the rat. *J Comp Neurol.* 183:647-664.
- Donoghue JP, Parham C. 1983. Afferent connections of the lateral agranular field of the rat motor cortex. *J Comp Neurol.* 217:390-404.
- Donoghue JP, Wise SP. 1982. The motor cortex of the rat: cytoarchitecture and microstimulation mapping. *J Comp Neurol.* 212:76-88.
- Faull RLM, Carman JB. 1978. The cerebellofugal projections in the brachium conjunctivum of the rat. I. The contralateral ascending pathway. *J Comp Neurol.* 178:495-518.
- Freneau RT, Troyer MD, Pahner I, Nygaard GO, Tran CH, Reimer RJ, Bellocchio EE, Fortin D, Storm-Mathisen J, Edwards RH. 2001. The expression of vesicular glutamate transporters defines two classes of excitatory synapse. *Neuron.* 31:247-260.
- Fujiyama F, Furuta T, Kaneko T. 2001. Immunocytochemical localization of candidates for vesicular glutamate transporters in the rat cerebral cortex. *J Comp Neurol.* 435:379-387.
- Furuta T, Tomioka R, Taki K, Nakamura K, Tamamaki N, Kaneko T. 2001. In vivo transduction of central neurons using recombinant Sindbis virus: Golgi-like labeling of dendrites and axons with membrane-targeted fluorescent proteins. *J Histochem Cytochem.* 49:1497-1507.
- Gauthier-Campbell C, Bredt DS, Murphy TH, El-Husseini AE-D. 2004. Regulation of dendritic branching and filopodia formation in hippocampal neurons by specific acylated protein motifs. *Mol Biol Cell.* 15:2205-2217.
- Groenewegen HJ, Witter MP. 2004. Thalamus. In: Paxinos G, editor. *The rat nervous system.* 3rd ed. San Diego (CA): Elsevier. p. 407-453.
- Hall RD, Lindholm EP. 1974. Organization of motor and somatosensory neocortex in the albino rat. *Brain Res.* 66:23-38.
- Herzog E, Bellenchi GC, Gras C, Bernard V, Ravassard P, Bedet C, Gasnier B, Giros B, El Mestikawy S. 2001. The existence of a second vesicular glutamate transporter specifies subpopulations of glutamatergic neurons. *J Neurosci.* 21:U1-U6.
- Hioki H, Fujiyama F, Taki K, Tomioka R, Furuta T, Tamamaki N, Kaneko T. 2003. Differential distribution of vesicular glutamate transporters in the rat cerebellar cortex. *Neuroscience.* 117:1-6.
- Hoshi E, Tremblay L, Féger J, Carras PL, Strick PL. 2005. The cerebellum communicates with the basal ganglia. *Nat Neurosci.* 8:1491-1493.
- Ito T, Hioki H, Nakamura K, Tanaka Y, Nakade H, Kaneko T, Iino S, Nojo Y. 2007. Gamma-aminobutyric acid-containing sympathetic preganglionic neurons in rat thoracic spinal cord send their axons to the superior cervical ganglion. *J Comp Neurol.* 502:113-125.
- Jensen KF, Killackey HP. 1987. Terminal arbors of axons projecting to the somatosensory cortex of the adult rat. I. The normal morphology of specific thalamocortical afferents. *J Neurosci.* 7:3529-3543.
- Jinnai K, Nambu A, Yoshida S. 1987. Thalamic afferents to layer I of anterior sigmoid cortex originating from the VA-VL neurons with entopeduncular input. *Exp Brain Res.* 69:67-76.
- Jones EG. 1998. Viewpoint: the core and matrix of thalamic organization. *Neuroscience.* 85:331-345.
- Jones EG. 2001. The thalamic matrix and thalamocortical synchrony. *Trends Neurosci.* 24:595-601.
- Jones EG. 2007. *The thalamus.* 2nd ed. Cambridge (UK): Cambridge University Press.
- Kameda H, Furuta T, Matsuda W, Ohira K, Nakamura K, Hioki H, Kaneko T. 2008. Targeting green fluorescent protein to dendritic membrane in central neurons. *Neurosci Res.* 61:79-91.
- Kaneko T, Fujiyama F. 2002. Complementary distribution of vesicular glutamate transporters in the central nervous system. *Neurosci Res.* 42:243-250.
- Larkum ME, Senn W, Lüscher H-R. 2004. Top-down dendritic input increases the gain of layer 5 pyramidal neurons. *Cereb Cortex.* 14:1059-1070.
- McFarland NR, Haber SN. 2000. Convergent inputs from thalamic motor nuclei and frontal cortical areas to the dorsal striatum in the primate. *J Neurosci.* 20:3798-3813.
- McFarland NR, Haber SN. 2001. Organization of thalamostriatal terminals from the ventral motor nuclei in the macaque. *J Comp Neurol.* 429:321-336.
- McFarland NR, Haber SN. 2002. Thalamic relay nuclei of the basal ganglia form both reciprocal and nonreciprocal cortical connections, linking multiple frontal cortical areas. *J Neurosci.* 22:8117-8132.
- Mitchell BD, Cauller LJ. 2001. Corticocortical and thalamocortical projections to layer I of the frontal neocortex in rats. *Brain Res.* 921:68-77.
- Moriyoshi K, Richards LJ, Akazawa C, O'Leary DDM, Nakanishi S. 1996. Labeling neural cells using adenoviral gene transfer of membrane-targeted GFP. *Neuron.* 16:255-260.
- Nakamura K, Matsumura K, Hübschle T, Nakamura Y, Hioki H, Fujiyama F, Boldogkői Z, König M, Thiel H-J, Gerstberger R, et al. 2004. Identification of sympathetic premotor neurons in medullary raphe regions mediating fever and other thermoregulatory functions. *J Neurosci.* 24:5370-5380.
- Nakamura KC, Kameda H, Koshimizu Y, Yanagawa Y, Kaneko T. 2008. Production and histological application of affinity-purified antibodies to heat-denatured green fluorescent protein. *J Histochem Cytochem.* 56:647-657.
- Nakano K, Tokushige A, Kohno M, Hasegawa Y, Kayahara T, Sasaki K. 1992. An autoradiographic study of cortical projections from motor thalamic nuclei in the macaque monkey. *Neurosci Res.* 13:119-137.
- Oda S, Kishi K, Yang JL, Chen SY, Yokofujita J, Igarashi H, Tanihata S, Kuroda M. 2004. Thalamocortical projection from the ventral posteromedial nucleus sends its collaterals to layer I of the primary somatosensory cortex in rat. *Neurosci Lett.* 367:394-398.
- Paxinos G, Kus L, Ashwell KWS, Watson C. 1999. *Chemoarchitectonic atlas of the rat forebrain.* San Diego (CA): Academic Press.
- Paxinos G, Watson C. 2007. *The rat brain in stereotaxic coordinates.* 6th ed. London: Academic Press.
- Roland PE. 2002. Dynamic depolarization field in the cerebral cortex. *Trends Neurosci.* 25:183-190.
- Sakai ST, Grofova I, Bruce K. 1998. Nigrothalamic projections and nigrothalamocortical pathway to the medial agranular cortex in the rat: single- and double-labeling light and electron microscopic studies. *J Comp Neurol.* 391:506-525.
- Sasaki K, Gemba H. 1981. Cortical field potentials preceding self-paced and visually initiated hand movements in one and the same monkey and influences of cerebellar hemispherectomy upon the potentials. *Neurosci Lett.* 25:287-292.
- Sasaki K, Gemba H. 1982. Development and change of cortical field potentials during learning processes of visually initiated hand movements in the monkey. *Exp Brain Res.* 48:429-437.
- Sasaki K, Kawaguchi S, Matsuda Y, Mizuno N. 1972. Electrophysiological studies on cerebello-cerebral projections in the cat. *Exp Brain Res.* 16:75-88.
- Sasaki K, Kawaguchi S, Oka H, Sakai M, Mizuno N. 1976. Electrophysiological studies on the cerebello-cerebral projections in monkeys. *Exp Brain Res.* 24:495-507.
- Sasaki K, Staunton HP, Dieckmann G. 1970. Characteristic features of augmenting and recruiting responses in the cerebral cortex. *Exp Neurol.* 26:369-392.

- Sawyer SF, Tepper JM, Groves PM. 1994. Cerebellar-responsive neurons in the thalamic ventroanterior-ventrolateral complex of rats: light and electron microscopy. *Neuroscience*. 63:725-745.
- Sawyer SF, Young SJ, Groves PM. 1989. Quantitative Golgi study of anatomically identified subdivisions of motor thalamus in the rat. *J Comp Neurol*. 286:1-27.
- Shinoda Y. 1987. General discussion 3 in motor areas of the cerebral cortex. In: Paxinos G, editor. *Ciba Foundation Symposium 132*. New York: Wiley. p. 221-230.
- Shinoda Y, Kakei S. 1989. Distribution of terminals of thalamocortical fibers originating from the ventrolateral nucleus of the cat thalamus. *Neurosci Lett*. 96:163-167.
- Sholl DA. 1953. Dendritic organization in the neurons of the visual and motor cortices of the cat. *J Anat*. 87:387-406.
- Strick PL, Sterling P. 1974. Synaptic termination of afferents from the ventrolateral nucleus of the thalamus in the cat motor cortex. A light and electron microscope study. *J Comp Neurol*. 153:77-106.
- Tamamaki N, Nakamura K, Furuta T, Asamoto K, Kaneko T. 2000. Neurons in Golgi-stain-like images revealed by GFP-adenovirus infection in vivo. *Neurosci Res*. 38:231-236.
- Wang Y, Kurata K. 1998. Quantitative analyses of thalamic and cortical origins of neurons projecting to the rostral and caudal forelimb motor areas in the cerebral cortex of rats. *Brain Res*. 781:137-147.
- Yamamoto T, Kishimoto Y, Yoshikawa H, Oka H. 1990. Cortical laminar distribution of rat thalamic ventrolateral fibers demonstrated by the PHA-L anterograde labeling method. *Neurosci Res*. 9:148-154.
- Yamamoto T, Kishimoto Y, Yoshikawa H, Oka H. 1991. Intracellular recordings from rat thalamic VL neurons—a study combined with intracellular staining. *Exp Brain Res*. 87:245-253.